JOURNAL OF Applied Polymer SCIENCE

# Preparation and performance analysis of barium titanate incorporated in corn starch-based polymer electrolytes for electric double layer capacitor application

**K. H. Teoh, Chin-Shen Lim, Chiam Wen Liew, S. Ramesh**

Centre for Ionics University of Malaya, Department of Physics, Faculty of Science, University of Malaya, Lembah Pantai, Kuala Lumpur 50603, Malaysia

Correspondence to: S. Ramesh (E-mail: rameshtsubra@gmail.com)

**ABSTRACT:** Polymer electrolyte membranes composing of corn starch as host polymer, lithium perchlorate ($LiClO_4$) as salt, and barium titanate ($BaTiO_3$) as composite filler are prepared using solution casting technique. Ionic conductivity is enhanced on addition of $BaTiO_3$ by reducing the crystallinity and increasing the amorphous phase content of the polymer electrolyte. The highest ionic conductivity of $1.28 \times 10^{-2}$ S cm$^{-1}$ is obtained for 10 wt % $BaTiO_3$ filler in corn starch-$LiClO_4$ polymer electrolytes at 75°C. Glass transition temperature ($T_g$) of polymer electrolytes decreases as the amount of $BaTiO_3$ filler is increased, as observed in differential scanning calorimetry analysis. Scanning electron microscopy and thermogravimetric analysis are employed to characterize surface morphological and thermal properties of $BaTiO_3$-based composite polymer electrolytes. The electrochemical properties of the electric double-layer capacitor fabricating using the highest ionic conductivity polymer electrolytes is investigated using cyclic voltammetry and charge-discharge analysis. The discharge capacitance obtained is 16.22 F g$^{-1}$. © 2015 Wiley Periodicals, Inc. J. Appl. Polym. Sci. **2016**, *133*, 43275.

**KEYWORDS:** biopolymers & renewable polymers; composites; differential scanning calorimetry (DSC); thermogravimetric analysis (TGA)

Received 9 October 2015; accepted 28 November 2015

**DOI: 10.1002/app.43275**

## INTRODUCTION

Electrochemical capacitors have attracted much interest as alternative energy storage systems compared to conventional capacitors and secondary batteries in the last decade.[1–5] Electric double layer capacitors (EDLCs) are being developed in many research laboratories as alternative power sources. EDLCs have been widely used because of their advantageous properties such as free of maintenance and toxic free. EDLCs exhibit larger capacitance, higher specific power and longer cycle life over lithium batteries.[6–8] However, most EDLCs are developed using liquid electrolyte. Liquid electrolytes have higher conductivity and can deliver larger currents when in use, nevertheless the bulky design and leak prone nature has forced researchers to seek for an alternative way to solve the shortcomings.

Solid polymer electrolytes (SPEs) have been intensively studied since their discovery.[9] SPEs are of great interest due to their wide range of application and ease of preparation. SPEs have many advantages such as high specific energy, solvent-free, wide electrochemical stability window, and ease of processability.[10] However, low ionic conductivity of SPEs has drawn the attention of many researchers in order to improve their ionic conductivity. The common approach for increasing the ionic conductivity of SPEs is adding plasticizer into the polymer matrix, but this plasticizer can reduce the mechanical properties of SPEs.[11] One effective way of reducing the crystallinity of host polymer and improving ionic conductivity significantly in SPEs is incorporating nanofillers in the polymer electrolyte bulk which act as solid plasticizer. Dispersion of inert inorganic oxide such as $Al_2O_3$, $TiO_2$, ZnO, and $SiO_2$ has become an alternative approach, which has attracted considerable attention. Croce *et al.*[12] reported an increase in ionic conductivity by a magnitude of 3 orders on addition of low particle size ceramic powder.

Addition of inert ceramic fillers shows improvement in ionic conductivity, mechanical properties, and interfacial stability with various electrode materials. Various researches have been done to investigate the size of $BaTiO_3$ fillers toward the ionic conductivity of polymer electrolytes due to the interesting properties of $BaTiO_3$.[13] Sun *et al.*[14] reported that the addition of

**Table I.** Designation of Corn Starch-$LiClO_4$:$BaTiO_3$ Composite Polymer Electrolyte Films[25]

| | Composition of corn starch-$LiClO_4$-$BaTiO_3$ | | | | |
|---|---|---|---|---|---|
| | Weight (g) | | | | |
| Designation | Corn starch | $LiClO_4$ | Weight percentage (wt %) | Weight (g) $BaTiO_3$ | Weight percentage (wt %) |
| Ba-0 | 0.600 | 0.400 | 100 | 0.000 | 0 |
| Ba-2 | 0.588 | 0.392 | 98 | 0.020 | 2 |
| Ba-8 | 0.552 | 0.368 | 92 | 0.080 | 8 |
| Ba-10 | 0.540 | 0.360 | 90 | 0.100 | 10 |

ferroelectric material, $BaTiO_3$ increased the electrical conductivity and decreased the interfacial resistance between lithium anode and polymer electrolyte.

In recent years, clean, efficient energy production, and storage have taken the center stage in energy research. The rampant increase in renewable energy has put a demand on cheaper, safer, and more efficient storage devices. Natural polymers such as chitosan, starch, and cellulose pectin have attracted attention to be used as electrolyte in energy conversion and storage devices due to their wide availability, renewable, cost effective, and superior electrical properties.[15–19]

In view of this, corn starch has been used to develop solid biopolymer electrolytes, electrode materials, and starch-based biodegradable film.[20–22] The incorporation of ionic liquid into corn starch-based polymer electrolyte has exhibited superior ionic conductivity up to $10^{-2}$ S $cm^{-1}$.[23] Xiong *et al.*[24] reported that the addition of nano silicon dioxide (nano-$SiO_2$) into the polymer blends consisting of PVA and corn starch increased the water resistance and mechanical properties of the film.

This study aims to probe the effect of filler concentration on variations in ionic conductivity, surface morphology, and glass transition temperature in the series of corn starch-$LiClO_4$ polymer electrolytes. The conductivity results which are in good agreement with scanning electron microscopy (SEM) images, differential scanning calorimetry (DSC), and thermogravimetric analysis (TGA) data propose a new ion migration mechanism and ion interaction within polymer matrix. EDLC utilizing the highest ionic conductivity film will be fabricated and analyzed with cyclic voltammetry and charge-discharge analysis in this work.

## EXPERIMENTAL

### Materials and Characterizations

Corn starch was obtained from Sigma Aldrich and lithium perchlorate salt, $LiClO_4$, with 99.99% purity was obtained from Aldrich. Inorganic filler barium titanate, $BaTiO_3$ (Aldrich) was used to prepare composite polymer electrolyte by solution casting technique. Appropriate amount of corn starch, $LiClO_4$, and $BaTiO_3$ were dissolved in distilled water. The solution was then stirred for 24 h to ensure complete dissolution and homogeneity of mixture. The solution was then cast on Petri dish and dried in an oven to obtain a free standing composite polymer electrolyte. Table I shows the composition and designation of composite polymer electrolytes. The prepared composite polymer films were subjected to ac-impedance spectroscopy. Impedance spectroscopy was measured using HIOKI 3531-50 LCR Hi-Tester connected to a computer for data acquisition over the frequency range of 50 Hz–5 MHz at ambient temperature. For temperature dependence-ionic conductivity study, the ionic conductivities were measured from ambient temperature up to 75°C. Morphology of composite polymer electrolyte was studied by using Leica's SEM (model S440) at an acceleration potential of 8 kV at room temperature. Images were captured by automatic image capturing software. Magnifications are as indicated at the bottom of each figure. Thermal properties were studied using TA instrument thermal analyzer comprised of DSC Q200. Before analysis, the samples were equilibrated at 105°C for 5 min to remove any trace of water. The samples were then cooled rapidly to −50°C and then reheated to 200°C at a heating rate of 30.00°C $min^{-1}$. TGA were conducted with TA Q500 thermogravimetric analyzer under nitrogen atmosphere at a heating rate of 50°C $min^{-1}$. A 50 × 50 $mm^2$ polymer sheet film was soaked in distilled water for 5 min and the weights of the dried samples ($W_0$) were measured. Subsequently, the swollen samples were dried and placed in a desiccator until a constant weight was obtained ($W_1$) and the water solubility ($W_s$) was calculated using the following equation:

$$W_s = \frac{W_0 - W_1}{W_0} \times 100\%$$

### Preparation of EDLC

The electrodes for EDLC were prepared by mixing a ratio of 8 : 1 : 1 of activated carbon (BP20) purchased from SANWA Components, Inc : carbon black (Super P) : poly(vinylidine fluoride) (PVdF) in *N*-methylpyrrolidone (NMP) solvents. The mixture is allowed to stir until homogeneous slurry was obtained. The slurry was doctor-bladed on an aluminum foil current collectors. EDLC was constructed by sandwiching the most conducting polymer electrolyte between two activated carbon electrodes. Constructed EDLC cells were pressed under 200 mbar pressure to ensure good contact between electrode and polymer electrolyte film.

### EDLC Characterization

Linear sweep voltammetry (LSV) is used to determine the electrochemical stability window of the electrolyte. The CH-Instrument Model 600D electrochemical analyzer was used. The

**Table II.** Ionic Conductivity of the Composite Polymer Electrolytes at 25 and 75°C

| Samples | Ionic conductivity at 25°C (S $cm^{-1}$) | Ionic conductivity at 75°C (S $cm^{-1}$) |
|---|---|---|
| Ba-0 | $1.55 \times 10^{-6}$ | $1.28 \times 10^{-4}$ |
| Ba-2 | $4.58 \times 10^{-6}$ | $5.09 \times 10^{-3}$ |
| Ba-8 | $2.08 \times 10^{-5}$ | $1.01 \times 10^{-2}$ |
| Ba-10 | $1.84 \times 10^{-4}$ | $1.28 \times 10^{-2}$ |

electrolytes were sandwiched between stainless steel blocking electrodes and the measurements were performed in the range of −4 V to 4 V with a 10 $mVs^{-1}$ scan rate. Cyclic voltammetry (CV) was carried out using Autolab PGSTAT12 potentiostat-galvanostat from 0 to 1 V at 10 $mVs^{-1}$. Galvonostatic charging-discharging test was performed in the voltage range between 0 and 1 V at a constant current of 0.5 mA by using Neware battery cycler.

## RESULTS AND DISCUSSION

### Temperature Dependence Ionic Conductivity Studies

The temperature dependence conductivities of composite polymer electrolyte films were investigated at temperature range of 25–75°C. Table II shows the ionic conductivity of all composite polymer electrolytes at 25 and 75°C. Upon introduction of $BaTiO_3$, an abrupt increase in ionic conductivity is observed. The ionic conductivity of polymer electrolytes also increases with the mass fraction of fillers, from $4.58 \times 10^{-6}$ S $cm^{-1}$ (for Ba-2) to $2.08 \times 10^{-5}$ S $cm^{-1}$ (for Ba-8) and $1.84 \times 10^{-4}$ S $cm^{-1}$ (for Ba-10). This observation is accounted to the dissociation of $LiClO_4$ in corn starch matrix by weakening the inter-ion Coulomb force between the anions and cations, making more availability of $Li^+$ ions. This is mainly due to the ferromagnetism nature of $BaTiO_3$, which promotes faster dissociation of $LiClO_4$ salt. The general expression of ionic conductivity of a homogeneous polymer electrolyte is shown as

$$\sigma(T) = \Sigma n_i q_i \mu_i$$

where $n_i$ = number of charge carrier

$q_i$ = charge of ion

$\mu_i$ = mobility of ion

Based on the equation, mobility of charge carriers is the main feature that could affect the ionic conductivity. It should be noted that the amount of salt added in this composite polymer electrolyte system is the same. Therefore, the ionic conductivity is strongly controlled by the mobility and number of charge carriers. The ionic conductivity increases gradually with the concentration of $BaTiO_3$ added into the polymer complexes. Dispersion of $BaTiO_3$ promotes decoupling of lithium salt, increases the amount of charge carriers and eventually leads to higher ionic conductivity compared to filler-free polymer elecrolyte.

The ionic conductivity of polymer electrolytes has been increased about two orders of magnitude from $1.55 \times 10^{-6}$ to $1.84 \times 10^{-4}$ S $cm^{-1}$ at ambient temperature by adding 10 wt % of $BaTiO_3$. This can be explained by the effect of amylose and amylopectin segregation and the electrostatic forces originated from the dipole moments in the $BaTiO_3$ particles. Owing to its acidic surface, $BaTiO_3$ competes with the cations to interact with the basic ether oxygen of the polymer matrix. As a consequence, the ionic coupling of the oxygen with cation is reduced which promotes faster dissociation of the salt. The spontaneous polarization of $BaTiO_3$ facilitates salt dissociation which causes a highly conductive layer to form around $BaTiO_3$ particles and thus creates extra pathways for ion migration. These interactions increase the content of free charge carriers in the electrolytes and enhance the ionic conductivity of the nanocomposite polymer electrolytes.

Figure 1 depicts the plot of logarithm of $\sigma$ against 1000/$T$. As can be seen, the ionic conductivity values of composite polymer electrolytes increase as the temperature increases. The ionic conductivity of the most conducting polymer electrolyte achieves the highest ionic conductivity of $1.28 \times 10^{-2}$ S $cm^{-1}$ at 75°C. This is attributed to the expansion of polymer matrix when temperature is increased. Expansion of polymer matrix produces free volume and unoccupied spaces for the ion migration. However, the conductivity data exhibits two distinct behaviors. Ba-0 and Ba-2 exhibit Arrhenius type behavior while Ba-8 and Ba-10 are expected to obey Vogel-Tamman-Fulcher (VTF) relation. The ionic conductivity increases with increasing temperature which promotes the ion hopping mechanism.[26] The temperature dependent-ionic conductivity plot is fitted with Arrhenius rule as shown below:

$$\sigma(T) = \sigma_0 \exp\left(\frac{-E_a}{kT}\right)$$

where $\sigma_o$ is the pre-exponential factor, $E_a$ is the activation energy, $k$ is the Boltzmann constant, and $T$ is absolute temperature.

Conductivity data for Ba-8 and Ba-10 shows two distinct regions marked by a sluggish transition around 50°C. A tendency of curvature is observed above the softening point and this is believed to obey the VTF relation. This non-linear VTF behavior is often attributed to the segmental motion-assisted ionic transport in the elastomeric rich phase. Addition of $BaTiO_3$ has altered the way of ion diffusion in the polymer

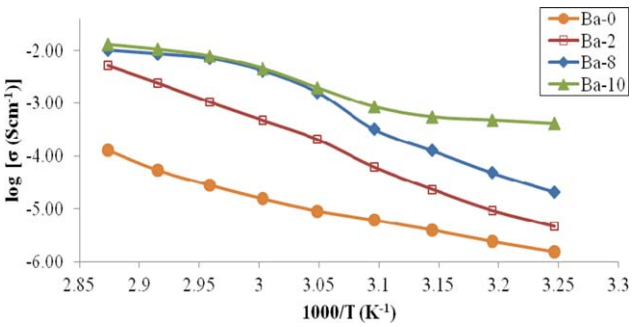


**Figure 1.** Variation of log conductivity as function of temperature change. [Color figure can be viewed in the online issue, which is available at wileyonlinelibrary.com.]

matrix. The obtained results comply with literature where addition of 10 wt % of $BaTiO_3$ into polymer electrolyte system shows VTF relation behavior.[13] We suggest that the increase in ionic conductivity at lower concentration of the filler particles is due to formation of Lewis acid-base interactions.[27] These interactions promote the dissociation of lithium salt and hence increase the number of mobile charge carriers.[28] On the other hand, formation of highly conductive pathway is favorable when more filler is added into the polymer electrolytes. The migrating ions can travel along this highly conducting pathway and eventually give rise to high ionic conductivity.

**SEM Studies**

SEM images of polymer electrolytes are shown in Figure 2(a–c). From the image of Ba-0 in Figure 2(a), distribution of $LiClO_4$ spread evenly on the surface of corn starch. The particle size of $LiClO_4$ is around 4–7 $\mu$m. However, when nanosized $BaTiO_3$ is introduced into the polymer matrix, $LiClO_4$ tend to aggregate to form a larger particle. As shown in Figure 2(b), Ba-2 shows a large aggregate particle where its grain size is around 25 $\mu$m. Dispersion of $BaTiO_3$ penetrates the polymer electrolyte system and dissociates excess $LiClO_4$, which adsorbs on the surface of polymer electrolyte. The salt dissociation resulting from addition of $BaTiO_3$ particles has formed a large conductive aggregate which provides extra pathway for ion migration.[14] Consequently, the ionic conductivity is improved for composite polymer electrolyte.

Ba-10 shows homogeneous distribution of $BaTiO_3$-$LiClO_4$ aggregate particles on the surface of corn starch. $LiClO_4$ will have more platforms to form complexation as more $BaTiO_3$ is added into the polymer electrolyte system. Ba-2 illustrates a few aggregates only around the surface of corn starch due to the lesser amount of $BaTiO_3$ in the system. However, Ba-10 shows a large and thick aggregate formation where there is an agglomeration of filler particles at high concentration of $BaTiO_3$.[27] The interaction between ionic species and fillers on the surface is responsible for the increase in ionic conductivity of polymer electrolytes. This is due to the creation of additional sites for ionic migration. Close inspection of Ba-10 morphological behavior explores the presence of tail like chain segments on the particles. This is responsible for the high ionic conductivity of the samples.[29]

**Thermal Analysis**

Thermal properties such as glass transition temperature ($T_g$), and melting temperature of crystalline phase ($T_m$) of the polymer electrolytes system can be evaluated from the DSC. The results are summarized in Table III. A drop in $T_g$ from 64.4°C for Ba-0 to 17.8°C for Ba-2 is observed. This is a suggestive of an enhancement in the flexibility of polymer chain. We suggest that doping of fillers can improve the segmental flexibility of polymeric chains within the electrolytes in which fillers can act as solid plasticizers. It is noteworthy to see that the most conducting polymer electrolyte exhibits the lowest $T_g$ value. This finding suggests that the addition of filler could increases the amorphous phase content of the polymer.[30]

Corn starch is mainly composed of two homopolymers which are amylose and amylopectin.[31] The $Li^+$ ions will attach to ether group on the amylase and amylopectin chain in the presence of $LiClO_4$. Addition of $BaTiO_3$ ceramic fillers influences the attraction of ether group on corn starch and $Li^+$ ion. $BaTiO_3$, a typical ferroelectric material with high dielectric

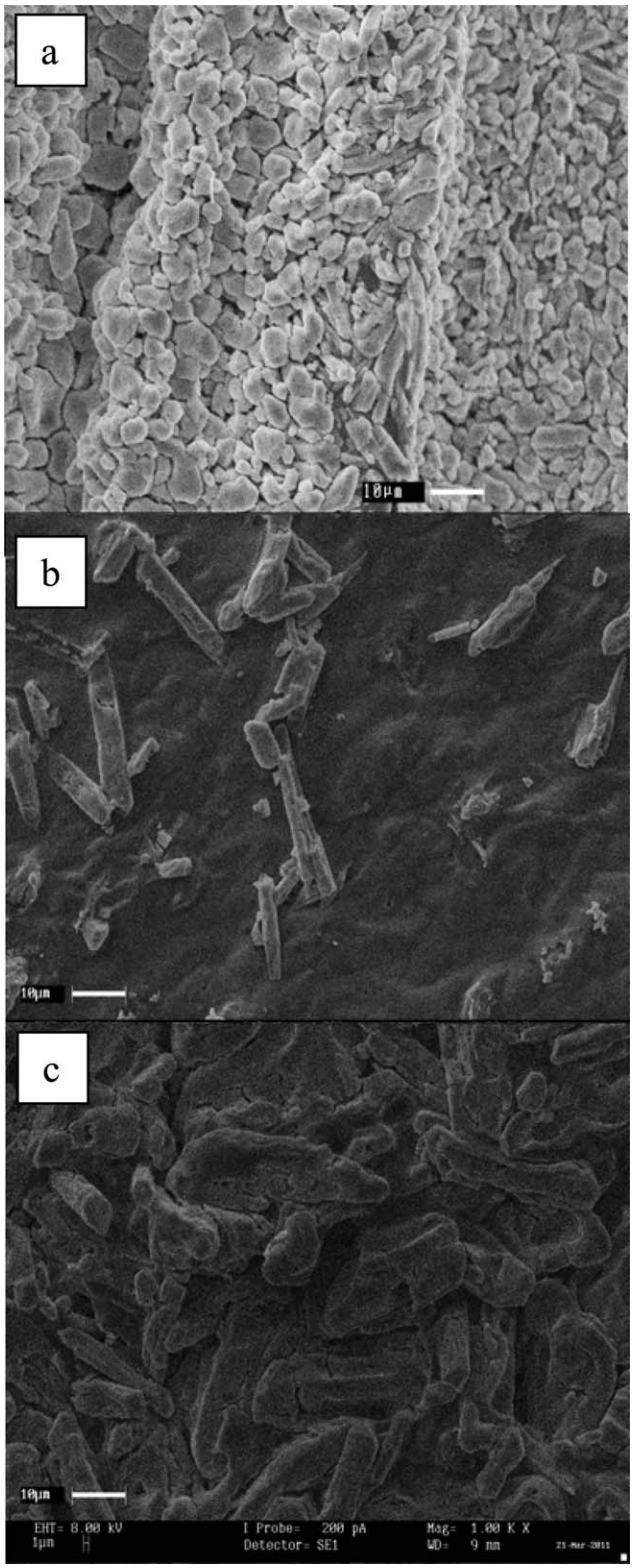


**Figure 2.** SEM images of (a) Ba-0, (b) Ba-2, and (c) Ba-10.

**Table III.** Thermal Properties and Water Solubilities of the Composite Polymer Electrolytes

| Samples | $T_g$ (°C) | $T_m$ (°C) | Decomposition temperature, $T_d$ (°C) | Water solubilities, $W_s$ (%) |
|---|---|---|---|---|
| Ba-0 | 64.4 | - | 237 | 50.44 |
| Ba-2 | 17.8 | 86.1 | 228 | 40.82 |
| Ba-8 | 17.4 | 84.9 | 259 | 20.45 |
| Ba-10 | 17.2 | - | 260 | 19.63 |

constant is dispersed in the amylose and amylopectin matrix. The electrostatic force originating from the dipole moments in the $BaTiO_3$ particles weakens the $Li^+$-O interaction in the carbohydrate polymer electrolyte chain.[32] Therefore, doping of filler creates extra migrating pathway for $Li^+$ ions due to the Lewis acid-base type interactions with O/OH surface group on $BaTiO_3$ grains. These interactions could be able to provide transient sites for ionic hopping and thus provide additional conductivity pathways for ion migration.[33] Figure 3 shows the crystallite melting temperature ($T_m$) of Ba-2, Ba-8, and Ba-10 in DSC thermogram. The endothermic peaks corresponding to the melting temperature of crystalline phase ($T_m$) are observed in Ba-2 and Ba-8. The occurrence of melting peak in the samples containing $BaTiO_3$ nanofillers could be rationalized to the trapping of water molecule crystal by the nanofiller or polymer-salt crystalline complexes.[34] The absence of endothermic peak in Ba-10 indicates that an amorphous phase is obtained.

TGA is carried out to investigate the decomposition temperature of the polymer film. The decomposition temperature of polymer electrolytes is decreased as small amount of $BaTiO_3$ is doped into corn starch polymer electrolytes. $BaTiO_3$ competes with the cation to interact with the basic ether oxygen of the polymer chains due to its ferromagnetic nature. Hence, cross-linked nature in corn starch matrix is reduced due to lesser amount of cations, which are available for the ion transportation. However, the decomposition temperature of the corn starch is found to be increased when more $BaTiO_3$ is introduced into the polymer electrolytes. The decomposition temperature for Ba-10 is increased from 228 to 260°C compared to Ba-2 as shown in Table III. From the obtained result, the weight loss has increased after excess addition of $BaTiO_3$ due to the saturated amount of filler particle in the polymer chain which restricts the segmental motion of the polymer. As we can seen from SEM microgram, the aggregates of fillers grain particles become larger in Ba-10 which is in good agreement with TGA results where Ba-10 shows the highest decomposition temperature. There is about 30% residue is remained after heating at 500°C. The remaining weight of the samples could be attributed to the residue of cross-linked polymer, lithium salt, and $BaTiO_3$ fillers.[35]

### Degree of Solubility

Solubility test is important to determine the water resistivity of the membrane. The hydrophilic nature of the hydroxyl group in amylose and amylopectin allows water absorption, causes the swelling of the membrane, and assists the ions permeation for transport through the membrane. However, the mechanical fragility and morphological instability of the polymer electrolyte membrane will be increased if too much water is absorbed on the electrolyte. Doping of $BaTiO_3$ into the system reduces the total weight loss percentage of the polymer membrane from 50.44% to 40.82% for Ba-0 and Ba-2, respectively. Ba-10 shows the lowest water solubility around 19.63%. Addition of ceramic fillers into the polymer system also reduces the penetration of water molecule into corn starch polymer. High concentration of fillers limits the polymer chain mobility and leads to a denser membrane structure as well as a smaller free volume which results in a smaller hydrophilic channel. The network structure formed through the complexation of $BaTiO_3$ with starch prevents the water molecules from dissolving and thereby improves the water resistance of the film.

### Linear Sweep Voltammetry

Linear sweep voltammetry is used to evaluate the working voltage of polymer electrolyte to be used in EDLC application. Figure 4 depicts the voltammogram of the most conducting composite polymer electrolyte, Ba-10. The electrochemical potential window of the most conducting polymer electrolyte lies in the range from −3.1 to 3.1 V. It can be observed that there are no appreciable current flows in the range of −3.1 to 3.1 V. Thus, this composite polymer electrolyte is stable up to 3.1 V for EDLC analysis.

### Performance Studies of EDLCs

CV is carried out to investigate the electrochemical behavior of charge storage at the interface of anodic and cathodic regions.[26] Figure 5 depicts the cyclic voltammograms of the EDLC for the first and 500th of charging and discharging processes at room temperature. The CV curve approaches to ideal rectangular shape where no redox peaks are observed. This can be attributed to the formation of a homogenous and ideally polarizable double layer formed at the interface.[36] The voltammograms exhibit almost perfect horizontal plateau indicating ion diffusion occurs at a fairly constant rate with minor impact from ohmic resistance.[37]

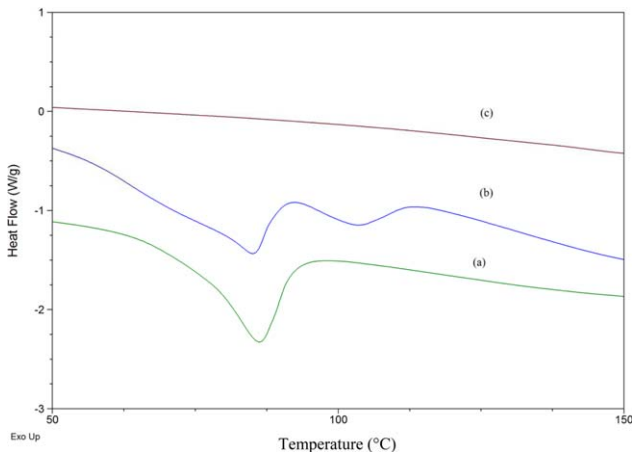


**Figure 3.** DSC thermogram of (a) Ba-2, (b) Ba-8, and (c) Ba-10 showing crystallite melting temperature. [Color figure can be viewed in the online issue, which is available at wileyonlinelibrary.com.]

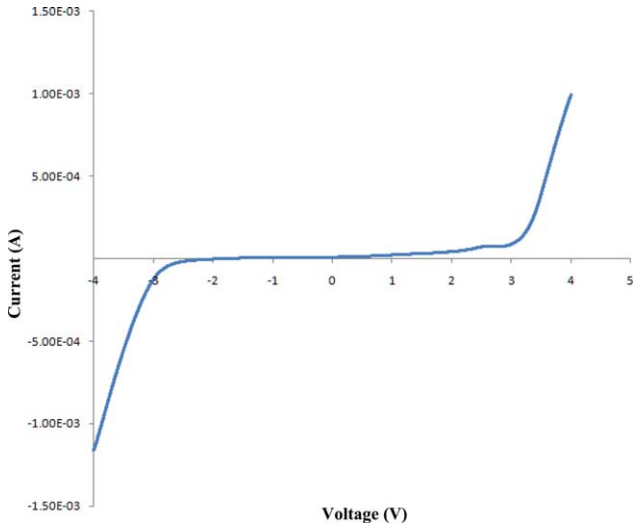


**Figure 4.** Linear sweep voltammetry of Ba-10 from −4 V to 4 V. [Color figure can be viewed in the online issue, which is available at wileyonlinelibrary.com.]

The charge-discharge characteristics of the EDLC cells are thus evaluated galvanostatically. Figure 6 shows the charge-discharge curves for the fabricated EDLC cell at current densities of 4.0 mA $cm^{-2}$ with a maximum cell potential of 1.0 V. The charge and discharge characteristics are found to be almost symmetrical. This indicates that the EDLC cell has high Coulombic efficiency. The initial jump/drop in the voltage during charging and discharging is observed. This observation arises from ohmic resistance (or referred as equivalent series resistance (ESR)) of the cell. The capacitance of the fabricated cell is deduced from the discharge curve using the equation below:

$$C = \frac{2\Delta I}{\Delta V \times m}$$

where $C$ is the capacitance of the cell (F $g^{-1}$), $\Delta I$ is the discharge current in amperes (A), $\Delta V$ is the voltage scan, and $m$ is

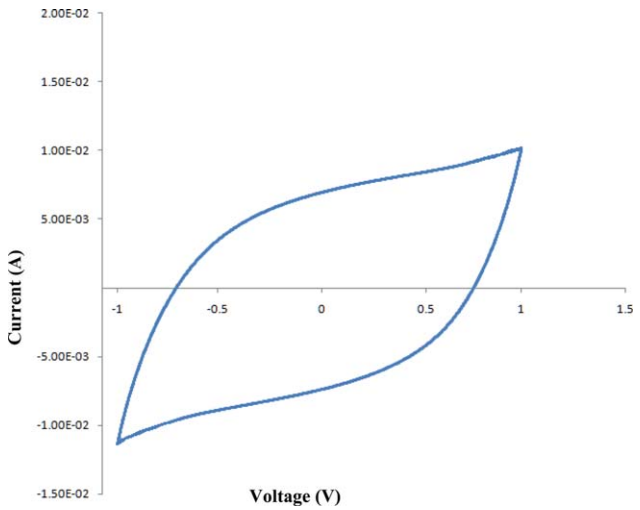


**Figure 5.** Cyclic voltammogram of EDLC fabricated from −1 V to 1 V. [Color figure can be viewed in the online issue, which is available at wileyonlinelibrary.com.]

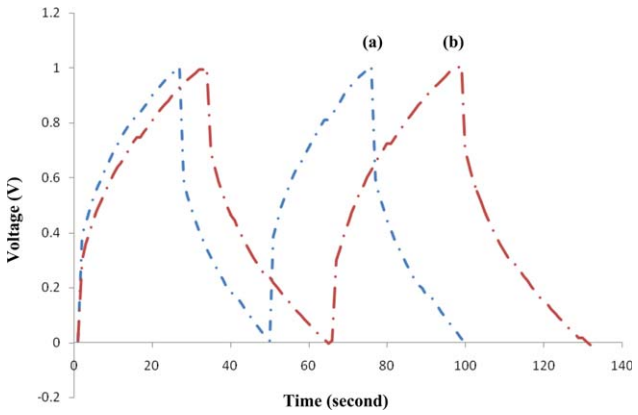


**Figure 6.** The charge-discharge curves for EDLC cell of (a) 1st cycle and (b) 500th cycle in the range of 0–1 V. [Color figure can be viewed in the online issue, which is available at wileyonlinelibrary.com.]

the mass of electrode. The capacitance calculated for the first charge-discharge cycle is 11.11 and 16.22 F $g^{-1}$ for the 500th cycle charge-discharge.

As depicted in Figure 7, the capacitance values have shown an increasing trend up to 300 cycles and stable up to 500 cycles. It could be due to the formation of Faradaic pseudo-capacity at the electrode and electrolyte interface. This Faradaic pseudo-capacity could reduce the resistance of ion migration and, therefore, improve the charge accumulation at the electrode-electrolyte boundary.[38] The proper formation of double layer charge on the surface of activated carbon reduces the ionic transfer resistance at the electrode-electrolyte interface and improves the EDLC performance. Long cycling tests is also performed to evaluate cycle durability of EDLC. Here we summarize the dependence of Coulombic efficiency on cycle number. Coulombic efficiency ($\eta$) is calculated as follows:

$$\eta = \frac{C_d}{C_c} \times 100\%$$

where $C_c$ and $C_d$ are the charge and discharge capacitance at each cycle, respectively. Fabricated EDLC cell shows good performance and maintained their Coulombic efficiency at ∼ 90% for 500 cycles. We propose that the excellent performance of the

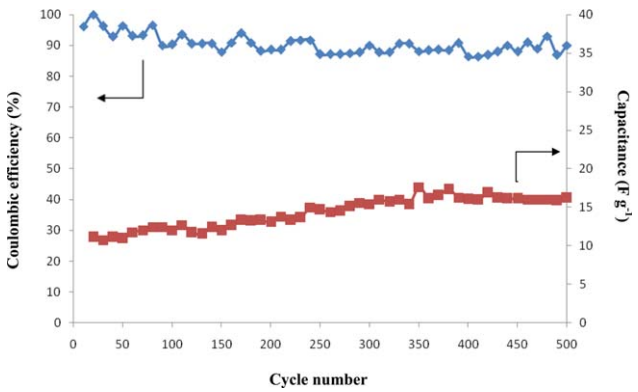


**Figure 7.** Variation of Coulombic efficiency and capacitance of EDLC cell as a function of cycle number. [Color figure can be viewed in the online issue, which is available at wileyonlinelibrary.com.]

**Table IV.** Capacitance of EDLCs using Different Solid Polymer Electrolytes

| Active material | Electrolytes | Working voltage (V) | Capacitance (F $g^{-1}$) | Reference |
|---|---|---|---|---|
| Carbon | Nafion/PTFE composite polymer | 0–2 | 16 | 39 |
| Activated carbon (BP20) | MC/$NH_4NO_3$/PEG200 | 0–0.85 | 38 | 40 |
| Carbon cloth | PU/EC/PC/$LiClO_4$ | 0–1 | 5.5 | 41 |
| Carbon black pearls 2000 | $(PEO\text{-}NPPP)_{11}/LiClO_4$ | 0–1 | 17 | 42 |
| Activated carbon (BP20) | Corn starch/$LiClO_4/BaTiO_3$ | 0–1 | 16.22 | This work |

cell is because of its proper interfacial contact between electrode and electrolyte and good electrochemical stability of the electrolyte. A comparison of the EDLC in this work with other studies is depicted in Table IV. Based on the literature, corn starch-based nanocomposite biopolymer electrolyte is a promising candidate to be applied in EDLC as this cell shows comparable and superior electrochemical performances.

## CONCLUSIONS

Addition of $BaTiO_3$ shows an increase in ionic conductivity by two orders of magnitude. Ba-10 shows the highest ionic conductivity of $1.28 \times 10^{-2}$ S $cm^{-1}$ at 75°C. The existence of extra migrating pathway is in good agreement with the data obtained from SEM and DSC analyses. DSC results show consistent $T_g$ values for all composite polymer electrolytes. Moreover, SEM images prove the homogeneous dispersion of fillers onto the polymer electrolytes. The incorporation of $BaTiO_3$ reduces the degree of swelling and increases the thermal stability of the composite polymer electrolytes. LSV confirms that the biopolymer electrolyte is stable up to 3.1 V. The EDLC cell consisting of the most conducting composite polymer electrolyte depicts the specific capacitance 16.22 F $g^{-1}$. The experimental data also indicates that the EDLC has excellent electrochemical stability and good cycle-life characteristics up to 500 cycles. The biodegradable composite polymer electrolyte is a promising material for solid-state supercapacitors.

## ACKNOWLEDGMENTS

This work was supported by the University of Malaya Research Grant (RP025A-14AFR) and Fundamental Research Grant Scheme (FP012-2015A) from Ministry of Higher Education, Malaysia.

## REFERENCES

1. Kim, K. S.; Park, S. J. *Microporous Mesoporous Mater.* **2012**, *163*, 140.
2. Tashima, D.; Yoshitama, H.; Sakoda, T.; Okazaki, A.; Kawaji, T. *Electrochim. Acta* **2012**, *77*, 198.
3. Sun, S. J.; Song, J.; Shan, Z. Q.; Feng, R. X. *J. Electroanal. Chem.* **2012**, *676*, 1.
4. Asmara, S. N.; Kufian, M. Z.; Majid, S. R.; Arof, A. K. *Electrochim. Acta* **2011**, *57*, 91.
5. Aravindan, V.; Reddy, M. V.; Madhavi, S.; Mhaisalkar, S. G.; Subba Rao, G. V.; Chowdari, B. V. R. *J. Power Sources* **2011**, *196*, 8850.
6. Burke, A. *J. Power Sources* **2000**, *91*, 37.
7. Kotz, R.; Carlen, M. *Electrochim. Acta* **2000**, *45*, 2483.
8. Yukari, K.; Takashi, S.; Mitsuyoshi, K.; Junji Atsushi, T. O. *J. Power Sources* **1996**, *60*, 219.
9. Fenton, D. E.; Parker, J. M.; Wright, P. V. *Polymer* **1973**, *14*, 589.
10. Kim, J. Y.; Kim, S. H. *Solid State Ionics* **1999**, *124*, 91.
11. Wu, X. L.; Xin, S.; Seo, H. H.; Kim, J. K.; Guo, Y. G.; Lee, J. S. *Solid State Ionics* **2011**, *186*, 1.
12. Croce, F.; Persi, L.; Ronci, F.; Scrosati, B. *Solid State Ionics* **2000**, *135*, 47.
13. Itoh, T.; Ichikawa, Y.; Uno, T.; Kubo, M.; Yamamoto, O. *Solid State Ionics* **2003**, *156*, 393.
14. Sun, H. Y.; Takeda, Y.; Imanishi, N.; Yamamoto, O.; Sohn, H. J. *J. Electrochem. Soc.* **2000**, *147*, 2462.
15. Colò, F.; Bella, F.; Nair, J. R.; Destro, M.; Gerbaldi, C. *Electrochim. Acta* **2015**, *174*, 185.
16. Bella, F.; Chiappone, A.; Nair, J. R.; Meligrana, G.; Gerbaldi, C. *Chem. Eng. Trans.* **2014**, *41*, 211.
17. Sharifi, F.; Ghobadian, S.; Cavalcanti, F. R.; Hashemi, N. *Renew. Sustainable Energy Rev.* **2015**, *52*, 1453.
18. Selvakumar, M.; Krishna Bhat, D. *J. Appl. Polym. Sci.* **2008**, *110*, 594.
19. Chupp, J.; Shellikeri, A.; Palui, G.; Chatterjee, J. *J. Appl. Polym. Sci.* **2015**, *132*, 42143.
20. Ramesh, S.; Liew, C. W.; Ramesh, K. *J. Non-Cryst. Solids* **2011**, *357*, 3654.
21. Li, Q. Y.; Wang, H. Q.; Dai, Q. F.; Yang, J. H.; Zhong, Y. L. *Solid State Ionics* **2008**, *179*, 269.
22. Lu, D. R.; Xiao, C. M.; Xu, S. J. *Express Polym. Lett.* **2009**, *3*, 366.
23. Wang, N.; Zhang, X. X.; Liu, H. H.; He, B. Q. *Carbohydr. Polym.* **2000**, *76*, 482.
24. Xiong, H. G.; Tang, S. W.; Tang, H. L.; Zou, P. *Carbohydr. Polym.* **2008**, *71*, 263.
25. Teoh, K. H.; Lim, C. S.; Ramesh, S. *Measurement* **2014**, *48*, 87.
26. Hashmi, S. A.; Kumar, A.; Tripathi, S. K. *J. Phys. D* **2007**, *40*, 6527.
27. Bhide, A.; Hariharan, K. *Polym. Int.* **2008**, *57*, 523.
28. Ulaganathan, M.; Pethaiah, S. S.; Rajendran, S. *Mater. Chem. Phys.* **2011**, *129*, 471.

29. Fan, L. Z.; Dang, Z. M.; Wei, G. D.; Nan, C.; Li, W. M. *Mater. Sci. Eng. B* **2003**, *99*, 340.

30. Johan, M. R.; Shy, O. H.; Ibrahim, S.; Yassin, S. M. M.; Hui, T. Y. *Solid State Ionics* **2011**, *196*, 41.

31. Pareta, R.; Edirisinghe, M. J. *Carbohydr. Polym.* **2006**, *63*, 425.

32. Takeuchi, T.; Ado, K.; Saito, Y.; Tabuchi, M.; Kageyama, H.; Nakamura, O. *Solid State Ionics* **1996**, *89*, 345.

33. Pitawala, H. J. M. C.; Dissanayake, M. A. K. L.; Seneviratne, V. A. *Solid State Ionics* **2007**, *178*, 885.

34. Marzantowicz, M.; Dygas, J. R.; Krok, F.; Florjanczyk, Z.; Zygadlo-Monikowska, E.; Lapienis, G. *Solid State Ionics* **2011**, *192*, 137.

35. Chung, H. J.; Woo, K. S.; Lim, S. T. *Carbohydr. Polym.* **2004**, *55*, 9.

36. Ganesh, B.; Kalpana, D.; Renganathan, N. G. *Ionics* **2008**, *14*, 339.

37. Tien, C. P.; Liang, W. J.; Kuo, P. L.; Teng, H. S. *Electrochim. Acta* **2008**, *53*, 4505.

38. Lewandowski, A.; Olejniczak, A. *J. Power Sources* **2007**, *172*, 487.

39. Subramaniam, C. K.; Ramya, C. S.; Ramya, K. *J. Appl. Electrochem.* **2011**, *41*, 197.

40. Shuhaimi, N. E. A.; Teo, L. P.; Woo, H. J.; Majid, S. R.; Arof, A. K. *Polym. Bull.* **2012**, *69*, 807.

41. Latham, R. J.; Rowlands, S. E.; Schlindwein, W. S. *Solid State Ionics* **2002**, *147*, 243.

42. Lavall, R. L.; Borges, R. S.; Calado, H. D. R.; Welter, C.; Trigueiro, J. P. C.; Rieumont, J.; Neves, B. R. A.; Silva, G. G. *J. Power Sources* **2008**, *177*, 652.